Simulation of Charpy test for different impact velocities

Simulation of Charpy test for different impact velocities

A E Musteață[1], C Pirvu[2], L Deleanu[1] and C Georgescu[1]

[1]Department of Mechanical Engineering, „Dunarea de Jos" University, Galati, Romania
[2]National Institute for Aerospace Research „Elie Carafoli" INCAS, Bucharest, Romania

E-mail: lorena.deleanu@ugal.ro

Abstract. This paper presents how a finite element model of Charpy sample fails when it is hit with an impactor. Studying the step-by-step evolution of failure of polymeric sample allows for establishing stages of the process characterising the Charpy impact, pointing out processes and phenomena that are difficult to be noticed during the actual impact or by investigating the broken pieces. The simulation was run for different impact velocities (1...3 m/s) and the sample material was considered a bilinear orthotropic hardening model. After analysing the images of the simulations, the following conclusions may be formulated. Simulation helps identifying the stages of the material failure. Using the bilinear hardening model for the polymer failure at low impact velocity (1...3 m/s) gave reasonable simulations. The time for failure process is longer at lower speed and the aspect of the failed surface depends on the impact velocity.

1. Introduction

The Charpy test was developed by Russell and Georges Charpy, at the beginning of the 20th century. It is one of the most common impact testing methods due to the simple shape of samples and the simplicity of the mechanical rig and thus, the results are easy to obtain and compare [1], [2]. The test rig consists of a weighted pendulum, which is dropped from a specified height to impact the sample. The energy consumed to deform or break the sample is simply calculated by the difference in the height of the pendulum, before and after the sample impact.

Procedures for Charpy testing are included in standards and the most preferred are ASTM E23, ASTM A370, ISO 148 or EN 10045-1. While the test has been most frequently performed on metallic materials, there are several standards applying for polymers, including ASTM D6110 and ISO 179.

Ductile crack initiation and propagation in Charpy specimens change the stress distribution ahead of the notch root. The stress level ahead of this notch root is significantly increased after ductile crack initiation. The quasi-static and dynamic formulations yield similar stress-strain distributions, confirming the results from the energy balance. Adiabatic heating, accounted for both the quasi-static and dynamic formulations, slightly favours crack initiation. The Gurson-Tvergaard-Needleman model allows a good failure prediction with strain rate and temperature independent damage parameters [3].

2. Model

The method of finite elements could help the engineer to avoid some unsolved issues in the analytical models. Many times, the transition from brittle to ductile fracture was described by experimental data that were, sometimes, misinterpreted [4]. The results of a Charpy test, especially the fracture energy on temperature, depend on structural parameters of the material. Polymers have complex structure and, thus, the influence of their structure on this curve is very peculiar, including aspects of composition, morphology and molecular structure. But these parameters are also inter-conditioned, so the problem

becomes more complicated.

A Charpy sample is typically a bar with a notch machined into one face (figure 1 presents the draw of the sample used in this simulation). The notch is placed on the opposite face to that bearing the impact and helps concentrate the stress and fracture initiation in the middle zone of the sample. Testing can be performed on a large temperature range. For this model, the impactor has 0.504 kg, this value being characteristic for Charpy test machine for polymers and the impact surface is plane. Its geometry is very close to that proposed in standards.

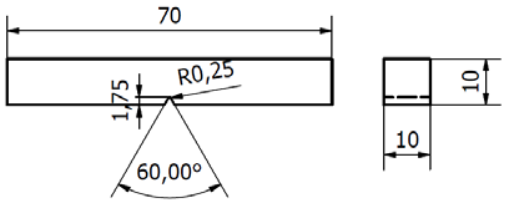

Figure 1. Dimension of the sample (for this simulation).

The authors used the code AutoDyn and the explicit Lagrangian dynamic solver. The materials being considered bilinear orthotropic with hardening, characterized by a yield strength and a tangential modulus. The failure criterion was considered the equivalent plastic strain thus, the failure occurs when this value is reached. The body erosion is controlled by the program and imposed by the same factor as for the other bodies in the model [5], based on the geometrical deformation limit, one for each material.

Shokrieh and Joneidi [6] designed the mesh of the Charpy specimen with three distinct regions: the region parallel with the contact surface is most refined in order to guarantee a good contact with the striker, the region around the notch is refined as the stress is concentrated at the notch tip and the rest of the material volume.

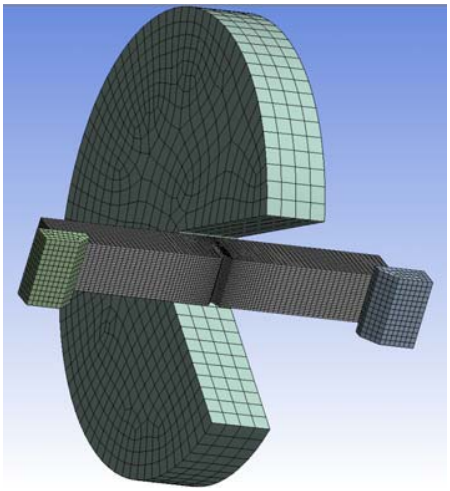

Figure 2. The model.

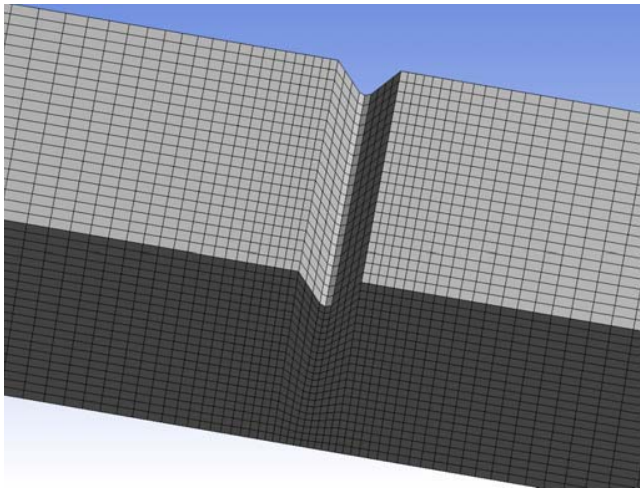

Figure 3. Detail of mesh in the notch zone.

The model has four bodies (figure 2), the polymeric sample and three bodies made of stainless steel (the impactor and two supports with round corners).

Rossol et al. [7] proposed the following initial and boundary conditions: striker velocity imposed, rate-dependent material behavior, quasi-static or fully dynamic (including inertia terms) solution procedure and adiabatic (not allowing any transfer of the heat generated by plastic deformation, since

the characteristic heat diffusion time is considered to be about one order of magnitude longer than the duration of an impact test).

The authors took into considerations the followings: adiabatic conditions at room temperature (22°C), imposed impact velocity. Also, they introduced friction between the impactor and the sample and between the rigid supports and the sample (COF = 0.25, a typical value for sliding contact polymer-metal). Even some recent papers [8], [9] neglect friction in their simulations. But other authors consider the friction between surfaces in contact. Ghaith and Khan [10] introduced in their model two types of frictional contact interactions; sample-support and impactor-sample.

The contact conditions are: the contact between the Charpy sample and its supports and also the contact between the polymeric sample and the impactor are considered friction contacts, characterised by a constant friction coefficient of 0.25. Boundary conditions refer to the supports with fixed surface ends, that is the nodes on the surfaces laying on the machine frame have no movement and no rotation. Initial conditions consider that the impactor velocity just before reaching the sample surface could vary, this paper presenting simulation results for impact velocity (v_0) of 1 m/s, 2 m/s and 3 m/s, characteristic for Charpy tests: 3.7 m/s [11], 5...9 m/s for steel modelling [12]. The mesh sensitivity depends on the element size that should be as smaller as possible and a finer mesh could be requested on the notch zone. For models with bodies with very different levels of dimensions (here, the sample and its bottom-round notch), the mesh presents some issues. An improved mesh will ask for a more performant computer. Minimum edge length is 0.5236 mm and the growth rate are set at 1.2. Element size is 0.4...0.7 mm (figure 3) for the notch zone (the radius of the notch being r = 0.25 mm). The maximum energy error is set for 0.9. The end time is set at 10^{-3} s.

Taking into account the narrow range of the impact velocity (1...3 m/s), this simulation was done for constitutive bilinear hardening polymeric material, similar to a polyethylene grade (table 1). An improved model may use constitutive models depending on strain rate and temperature, as that proposed by Johnson and Cook [13].

Table 1. Material characterization.

Property	**Polymer**	**Stainless steel**
Density, kg/m^3	950	7750
Young modulus, MPa	1100	193000
Poisson ratio	0.42	0.31
Bulk modulus, MPa	2291.7	169300
Shear modulus, MPa	387.32	73664
Yield strength, MPa	25	207 (compression and tensile)
Tangent modulus, MPa	350	
Maximum equivalent plastic strain	0.05	

3. Results

Figures 4, 5 and 6 present several moments of the failure process, pointing out that, even if the velocity range is not large (1...3 m/s), the behavior of the sample is quite different.

The difference in failure process may be point out by comparing the graphs in figures 9, 10, 11. At v_0 = 1 m/s, the maximum von Mises stress is reached after a longer time from the impact, $\Delta t = 1.75\times10^{-3}$ s. At v = 2 m/s, the maximum value is recorded at $\Delta t = 1.24\times10^{-3}$ s and at v_0 = 3 m/s, this time interval is $\Delta t = 1.0\times10^{-3}$ s. Sample impacted at v = 1 m/s is not yet totally broken (the sample is not yet split in two pieces). Thus, 10^{-5} s is not enough to simulate the failure at this speed and the high value of equivalent stress is a prove. It seems that the separation advances smoothly at slow velocity

and in steps at higher ones (see the several stress peaks for v_0 = 2 m/s and v_0 = 3 m/s and the peaks are sharper for the highest velocity.

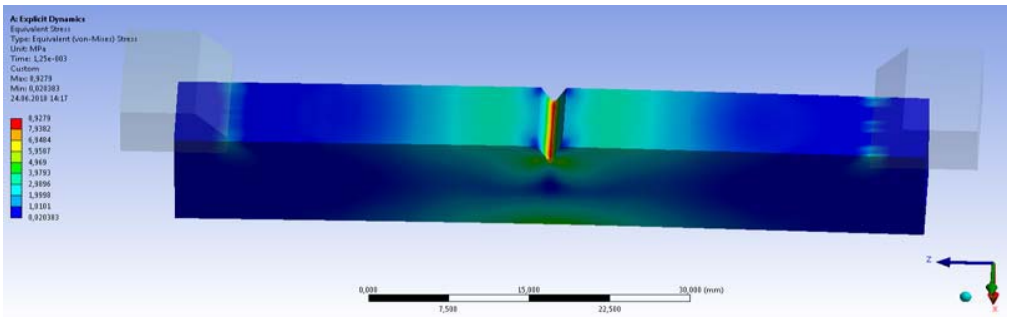

a) t = 1.25×10^{-3} s

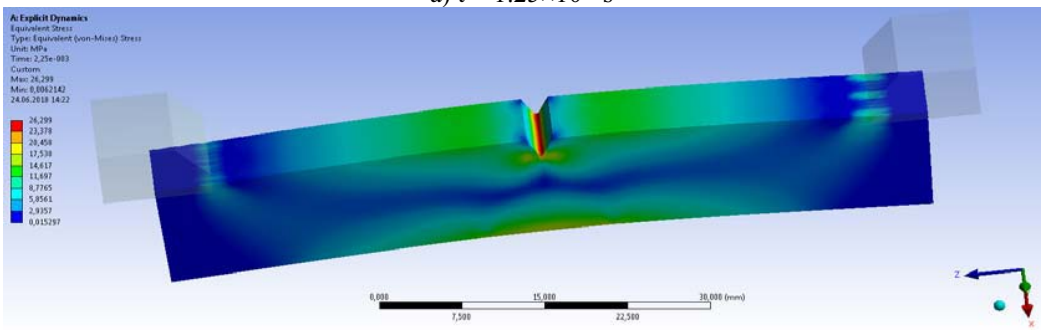

b) t = 2.25×10^{-3} s

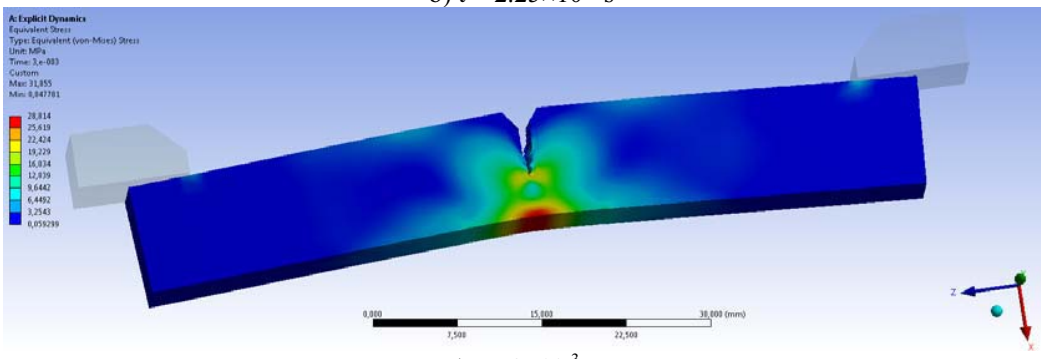

c) t = 3×10^{-3} s

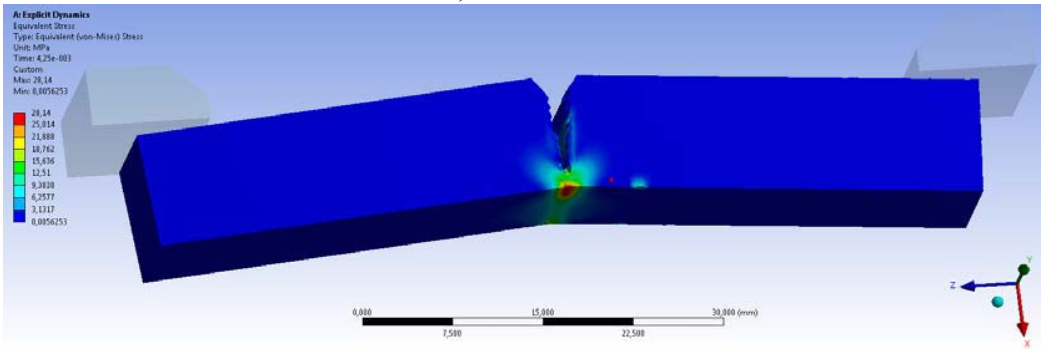

d) t = 4.25×10^{-3} s

Figure 4. Moments of failure for the impactor velocity of v_0 = 1 m/s (impact start at t = 1.0×10^{-3} s).

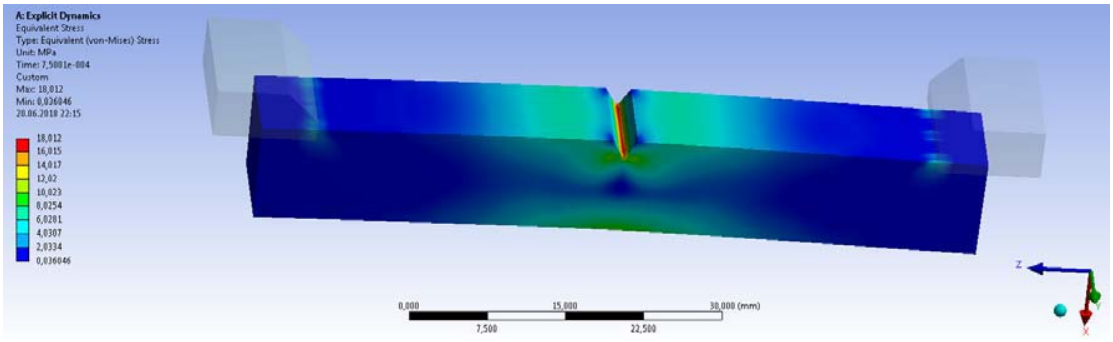

a) $t = 7.5\times10^{-4}$ s

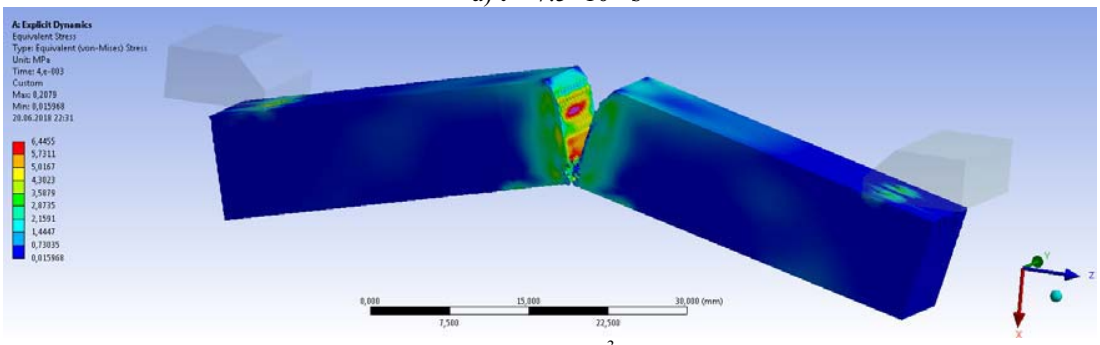

b) $t = 4\times10^{-3}$ s

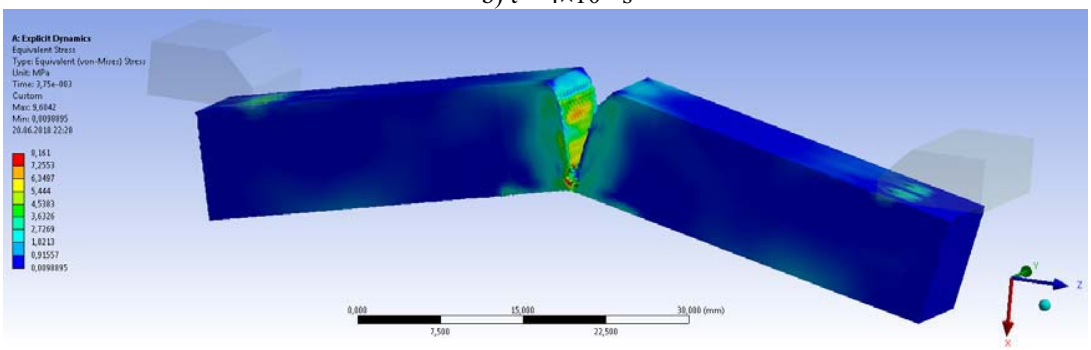

c) $t = 3.75\times10^{-3}$ s

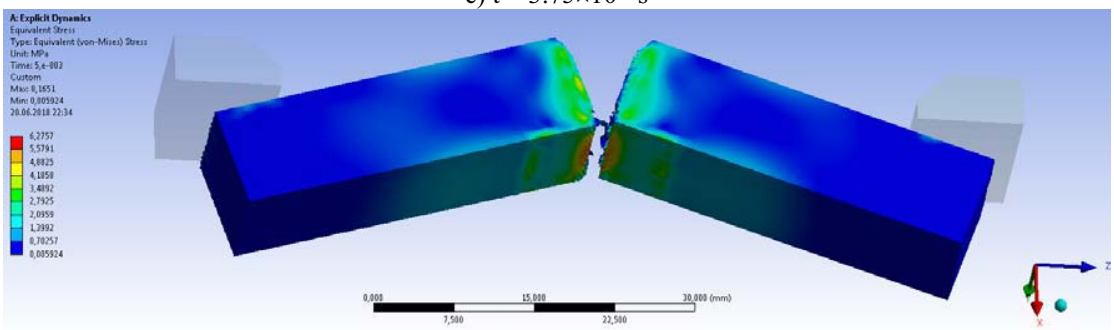

d) $t = 5\times10^{-3}$ s

Figure 5. Moments of the failure for the impactor velocity of $v_0 = 2$ m/s (impact start at $t = 5\times10^{-4}$ s).

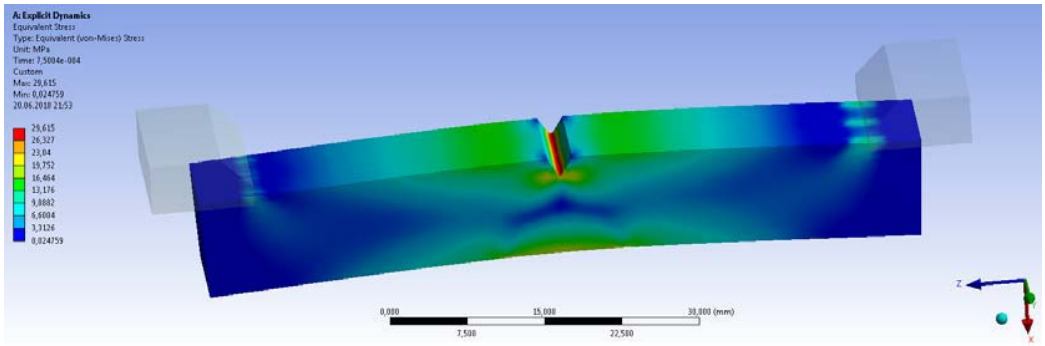

a) $t = 7.5\times10^{-4}$ s

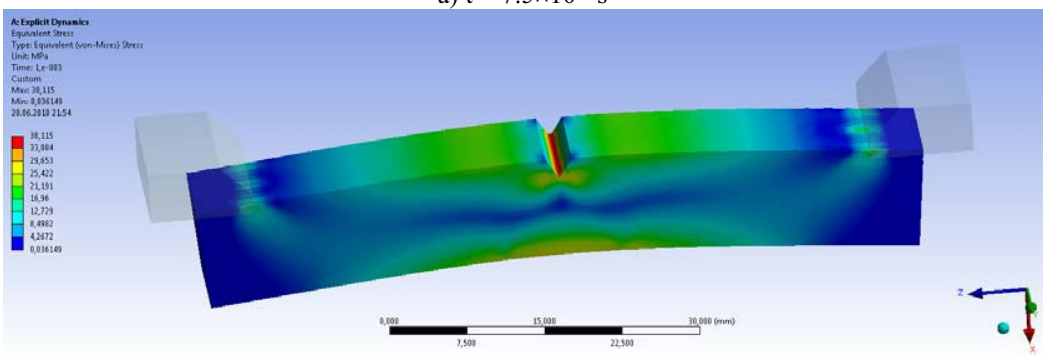

b) $t = 1\times10^{-3}$ s

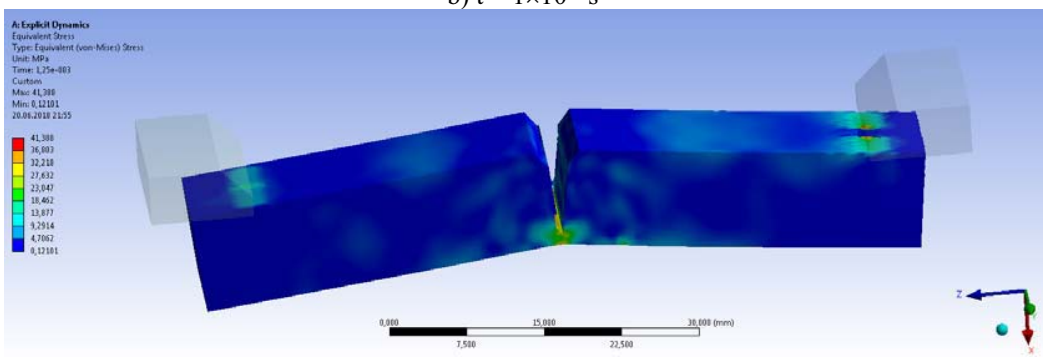

c) $t = 1.25\times10^{-3}$ s

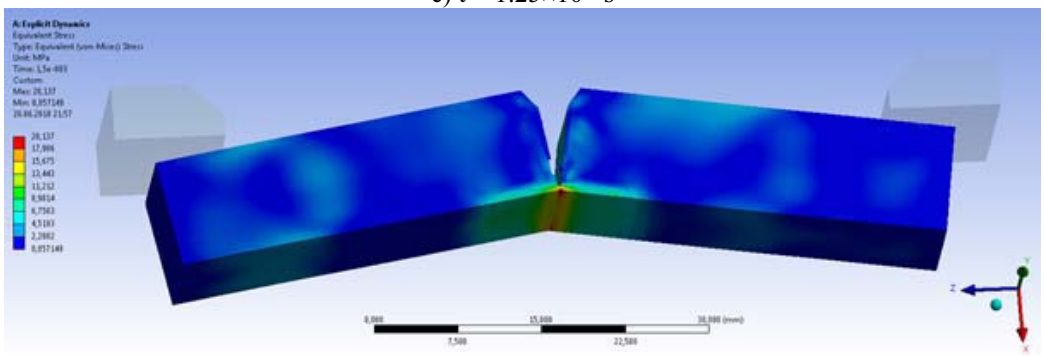

d) $t = 1.5\times10^{-3}$ s

Figure 6. Moments of the failure for the impactor velocity of $v_0 = 3$ m/s (impact start at $t = 2.5\times10^{-4}$ s).

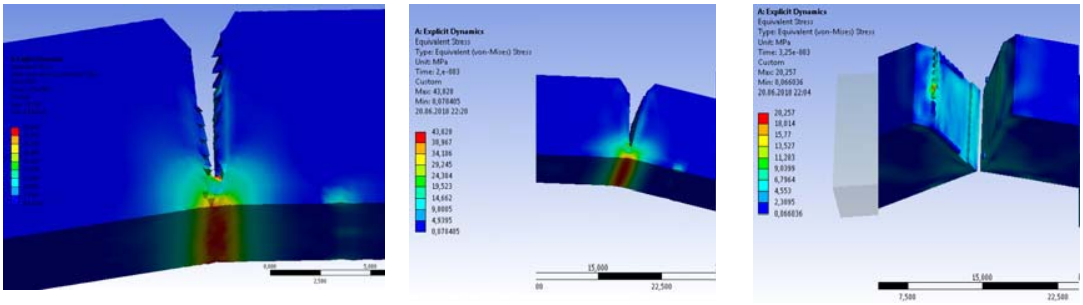

a) v_0 = 1 m/s, t = 3.75×10^{-3} s b) v_0 = 2 m/s, t = 2×10^{-3} s c) v_0 = 3 m/s, t = 3.25×10^{-3} s

Figure 7. Details of the sample failure for different impact initial velocity (von Mises stress distribution).

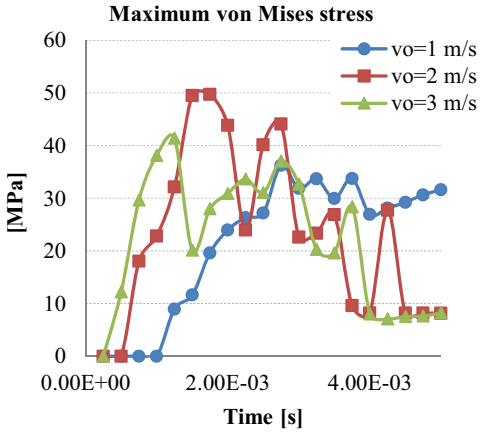

Figure 8. Maximum von Mises stress during the impact.

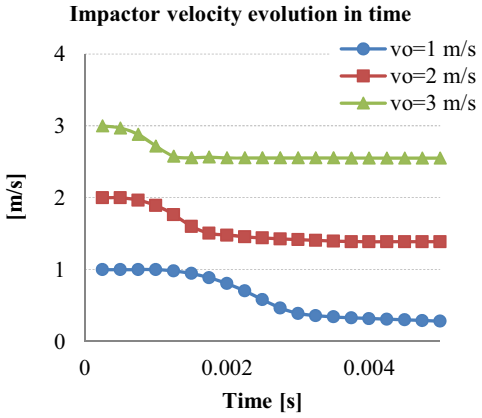

Figure 9. Impactor velocity during the impact.

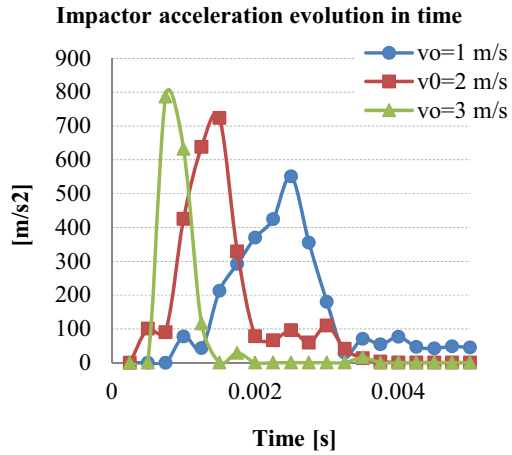

Figure 10. Impactor acceleration during the impact.

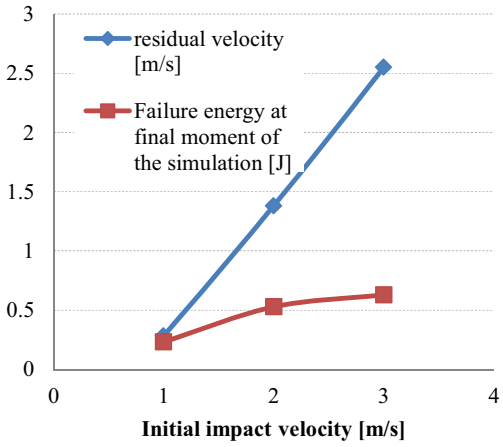

Figure 11. Residual velocity of the impactor and the failure energy at the final moment.

Acceleration has the highest value for the highest velocity, the peak is narrower than those at very low values. For v = 2 m/s, there is a small shoulder, explained by the elastic behavior of the material and than an increase on a larger time interval. Small oscillations are proving that breakage does not constantly advance, as one may see in figure 8. At lower impact velocity, the acceleration has a lower peak value, but larger shape. Very low values of acceleration (figure 10), a constant velocity (figure 9) and images in figure 7 suggest that the separation is almost finished for samples run at v = 2...3 m/s but it continues for v = 1 m/s. Same conclusion could be drawn from Figure 12. The energy spent for deformation and breakage is too small for accepting the separation of the two ends of the sample. But for the higher velocities, the energy "lost" for sample failure, in conjunction with the images in figures 9-11, differs with only 16% (taking into account the value for v = 3 m/s). Constitutive models from literature [14], [15], [16] also consider that higher strain rate makes the material more resistant.

The evolution of impactor velocity in time is similar for all velocities, but its decrease last shorter for a higher velocity.

A polymeric material tested by the authors (blend of PA6 + PP) has similar aspect (figure 12) with that obtained for the simulation with 1 m/s (figure 7.a and figure 4.d).

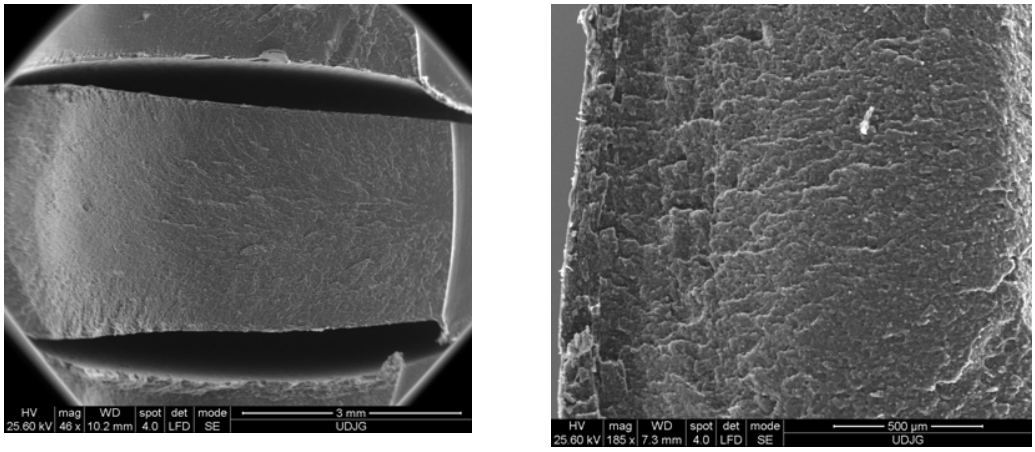

a) general view of the failed surface (edge of the notch zone is at right side of the image).

b) detail of the last failed zone (at the opposite surface to that containing the notch).

Figure 12. SEM images of a polymeric blend (PA + PP) tested by the authors at 1 m/s with an impactor of 0.5 kg.

4. Conclusions

After analysing the images of the simulations, the following conclusions may be formulated.

Simulation helps identifying the stages of the material failure.

Using the bilinear hardening model for the polymer failure at low impact velocity (1...3 m/s) gave reasonable simulations.

The time for failure process is longer at lower impact velocity and the aspect of the failed surface depends on this velocity.

5. References

[1] Holt J M 1990 *Charpy Impact Test: Factors and Variables* (Philadelphia: ASTM)
[2] Francois D and Pinneau A 2002 *From Charpy to present impact testing* (Oxford: Elsevier)
[3] Haušild P, Berdin C and Rossoll A 2005 Modelling of the Charpy impact test in the DBTT range *Materials Science Forum* **482** pp 331-334
[4] Bárányа T, Czigány T and Karger-Kocsis J 2010 Application of the essential work of fracture (EWF) concept for polymers, related blends and composites: A review *Progress in Polymer Science* **35** pp 1257–1287

[5] Năstăsescu V, Ştefan A and Lupoiu C 2001 *Analiza neliniară prin metoda elementelor finite. Fundamente teoretice şi aplicații* (Bucureşti: Academia Tehnică Militară)
[6] Shokrieh M M and Joneidi V A 2015 Characterization and simulation of impact behavior of graphene/ polypropylene nanocomposites using a novel strain rate–dependent micromechanics model *Journal of Composite Materials* **49** pp 2317–2328
[7] Rossoll A, Tahar M, Berdin C, Piques R, Forget P, Prioul C and Marini B 1996 Local Approach of the Charpy Test at Low Temperature *Journal de Physique IV Colloque* **06** pp C6-279-C6-286
[8] Mohan Kumar K, Devaraj M R and Lakshmi Narayana H V 2012 Finite element modelling for numerical simulation of Charpy impact test on materials *Proceedings of the International Conference on Challenges and Opportunities in Mechanical Engineering, Industrial Engineering and Management Studies ICCOMIM 2012* pp 32-36
[9] Serizawa H, Zhengqi W U and Murakawa H 2001 Computational analysis of Charpy impact test using interface elements *Transactions of JWRI* **30** pp 97-102
[10] Ghaith F A and Khan F A 2013 Three dimensional nonlinear finite element modeling of charpy impact test *International Journal of Mechanical Engineering and Technology* **4** pp 377-386
[11] Visser H A, Caimmi F and Pavan A 2013 Characterising the fracture toughness of polymers at moderately high rates of loading with the use of instrumented tensile impact testing *Engineering Fracture Mechanics* **101** pp 67–79
[12] Madhusudhan D, Chand S, Ganesh S and Saibhargavi U 2018 Modeling and simulation of Charpy impact test of maraging steel 300 using Abaqus *IOP Conf. Series: Materials Science and Engineering* **330** 012013
[13] Johnson G R and Cook W H 1985 Fracture characteristics of three metals subjected to various strains, strain rates, temperatures and pressures *Engineering Fracture Mechanics* **21** pp 31-48
[14] Capaldi F M 2012 *Continuum mechanics: constitutive modeling of structural and biological materials* (New York: Cambridge University Press)
[15] Puzrin A M 2012 *Constitutive Modelling in Geomechanics* (Heidelberg: Springer)
[16] Ottosen N S and Ristinmaa M 2005 *The mechanics of constitutive modeling* (Oxford: Elsevier)